siders homonuclear diatomic molecules formed from atoms containing ground state p electrons (e.g., Ne_2), the manifold of molecular states becomes so great that the necessary curve crossings for dissociative recombination can be expected to occur.

An extremely important result is the observation of Collins and Robertson[3,20] that the 10 830 Å (2^3P-2^3S) line does have a component which originates from He_2^+ in the afterglow, whereas all of the strong visible atomic lines originate from He^+, as demonstrated by the correlation of the intensities with molecular and atomic-ion distributions in flowing steady-state afterglow systems. Collins and Robertson calculate however that the contribution of dissociative (or collisional-dissociative) recombination which results in the 10 830 Å emission does not exceed $\alpha=2\times10^{-11}$ cm^3 sec^{-1} at 1800°K electron temperature. No reasonable extrapolation to 300°K can make this a significant contribution to the total electron recombination under ordinary laboratory conditions. Assuming $\alpha\approx T^{-3/2}$ leads to $\alpha(300°\text{K})<3\times10^{-10}$ cc sec^{-1} for example. The importance of the result lies in the fact that the mechanism for populating the 2^3P atomic state by electron recombination to the molecular ion is not apparent in the potential curves so far postulated.[21] An understanding of this experimental result thus offers promise of leading to new information concerning helium molecular potential states. In view of its importance, the experimental result should be carefully verified.

It might be pointed out that the observation of very complete molecular spectra of He_2 (in contrast to other rare gases for which molecular spectra are not observed) is presumably due in part to the fact that He_2^+ recombination is not dissociative, but rather leads to stable radiating He_2^* states. Members of the $n^3\Pi_g\rightarrow 2^2\Sigma_u^+$ Rydberg series with n as high as 15, have been observed in this laboratory, for example.

CONCLUSIONS

It seems reasonable to conclude that: (1) No convincing experimental evidence for dissociative recombination in He_2^+ which leads to visible light has as yet been reported. (2) No evidence for a large dissociative recombination coefficient exists and it appears that $\alpha_{DR}<3\times10^{-10}$ cm^3 sec^{-1}. (3) Theoretical explanations appear to exist. Recombination rates which have been measured in helium afterglows appear to be satisfactorily interpreted in terms of collisional-radiative recombination.

The combination of the new theoretical developments with the recently developed experimental technique of flowing afterglow systems can be expected to lead to substantial continued progress in understanding of the detailed mechanisms of helium and other afterglow systems.

ACKNOWLEDGMENTS

The authors wish to thank Professor Mulliken, Professor Takayanagi, Professor Robertson, Dr. Ginter, and Dr. Collins for manuscripts describing their investigations prior to publication.

This work has been supported in part by the Defense Atomic Support Agency.

PHYSICAL REVIEW VOLUME 138, NUMBER 2A 19 APRIL 1965

Elastic Resonances in Electron Scattering from He, Ne, Ar, Kr, Xe, and Hg†

C. E. KUYATT, J. AROL SIMPSON, AND S. R. MIELCZAREK
National Bureau of Standards, Washington, D. C.
(Received 16 November 1964)

The transmission of electrons through the rare gases and mercury vapor has been examined as a function of electron energy, with energy resolution of about 0.04 eV. Many anomalies (resonances) localized in energy have been observed, totaling 11 in helium, six in neon, two each in argon and krypton, five in xenon, and 13 in mercury. The interpretation of these resonances in terms of compound negative ion formation is discussed, and in several cases electron configurations are assigned to the negative ions. In helium, neon, xenon, and mercury, sharp decreases in transmission are observed which are attributed to the onset of inelastic processes. Definite identification of the inelastic processes in the case of helium permits calibration of the absolute electron energy scale to within ±0.03 eV.

INTRODUCTION

RECENT observations of sharp anomalies (resonances) in the electron total-scattering cross section and in the differential elastic-scattering cross section of atoms and molecules have shown the existence of highly excited states of the negative ions of these atoms and molecules. Schulz[1] observed the first such

† This research was supported in part by Project DEFENDER, sponsored by the Advanced Research Projects Agency, Department of Defense.

[1] G. J. Schulz, Phys. Rev. Letters **10**, 104 (1963). Schulz has also observed elastic resonances for electrons of about 1.5 to 3 eV in N_2: *Proceedings of the Sixth International Conference of Ionization Phenomena in Gases* (Paris, 1963), p. 41. These resonances are also ascribed to the formation of short-lived negative ion states, although the states appear to be of a somewhat different nature than the negative ion states to be discussed in this paper.

resonance in the elastic scattering of electrons from helium at 72°. The resonance appears as a sharp decrease in scattering for electrons near 19.3 eV, with an energy width much narrower than the energy resolution of the apparatus. In direct analogy with resonances observed in neutron scattering by nuclei, a resonance shows that a compound state exists at the resonance energy, the compound state having a relatively short lifetime for decay into the original components. In the case of electron scattering from helium, the compound state is a negative helium ion in a highly excited state, 19.3 eV above the ground state of the helium atom. Because the electrostatic field of the helium atom in its ground state is too weak to bind a third electron,[2] the negative helium ion has no stable state. [It does, however, have a metastable state,[3] $(1s2s2p)^4P_{5/2}$.]

Elastic scattering at 19.3 eV, being mainly s wave,[4–6] is approximately isotropic. If the sharp decrease in elastic scattering occurs at all angles, then the total elastic-scattering cross section should show a corresponding decrease. It follows that there should be a sharp increase in transmission of electrons through helium at 19.3 eV. This increase in transmission was demonstrated independently by Fleming and Higginson[7] and by Simpson.[8,9] The experiment of Fleming and Higginson employed relatively low resolution in energy and angle, while those of Simpson attained an energy resolution of about 0.05 eV, and an angular resolution of $\frac{3}{4}$°. Both demonstrated that there is a relatively transparent "window" in helium for electrons near 19.3 eV. Shortly thereafter, we demonstrated use of this narrow "window" as an electron monochromator and as an electron energy analyzer.[10]

The observation of the resonance in helium was quickly followed by the discovery of similar effects in neon. Schulz[11] observed one resonance near 16 eV in 72° elastic scattering, while Simpson[8,9] observed two sharp decreases in transmission near 16 eV. The apparent discrepancy is probably caused by a difference in energy resolution, since the two resonances are separated by only 0.1 eV. We have also reported a resonance with vibrational structure in molecular hydrogen.[12]

The resonances in helium and neon have been discussed by Simpson and Fano.[8] They picture the negative ion state responsible for the resonance as resulting from the addition of an electron to the lowest excited configuration of the atom with a binding energy of the order of 1 eV, and speculated that excited negative ions might result generally from the addition of an electron to the lowest configuration of atoms,[13] while addition of an electron to more highly excited configurations might be more difficult to observe. We have confirmed the prediction that elastic resonances are of widespread occurrence by observing such resonances in Ar, Kr, Xe, and Hg. In each case the strongest resonance or resonances are related to the lowest excited configuration of the atom. Furthermore, we have observed several resonances in He, Ne, and Hg which are based on more highly excited configurations of these atoms. Finally, in He, Ne, and Xe we have observed the inelastic component of the electron total-scattering cross section. The sharp rise at the threshold energy of the cross section for excitation of excited states of these atoms is associated with a decrease in transmitted current at the threshold energy.[14] These thresholds show promise as accurate calibration points for the determination of absolute electron energy scales.

METHOD OF OBSERVATION

Our method of observing resonances in total-scattering cross sections is identical in principle to the method introduced by Ramsauer[15] for the measurement of such cross sections. A well-collimated beam of electrons, with as narrow an energy spread as possible, is directed through a scattering chamber containing the gas to be investigated. The apparatus is designed so that electrons which are elastically scattered through more than a small angle or inelastically scattered, even without deflection, are lost from the beam and fail to arrive at the electron collector. Massey and Burhop[16] estimate that, to obtain an accuracy of 1% in the measured total-collision cross section, the maximum angle accepted by the electron detector must not exceed 11° at 1 eV, 6.5° at 10 eV, 2.3° at 100 eV, and 0.85° at 1000 eV, almost independently of the scattering gas. In our apparatus, electrons scattered more than 0.75° are lost to the beam, and the Massey and Burhop criterion is satisfied for electron energies less than 1000 eV. Preliminary experi-

[2] T. Y. Wu, Phil. Mag. **22**, 837 (1936).
[3] E. Holøien and J. Midtal, Proc. Phys. Soc. (London) **A68**, 815 (1955).
[4] C. Ramsauer and R. Kollath, Ann. Physik **12**, 529 (1932).
[5] H. S. W. Massey and E. H. S. Burhop, *Electronic and Ionic Impact Phenomena* (Clarendon Press, Oxford, 1956), Chap. III, Part 2.
[6] S. Westin, Kgl. Norske Videnskab. Selskabs Skrifter, No. 2 (1946).
[7] R. J. Fleming and G. S. Higginson, Proc. Phys. Soc. (London) **81**, 974 (1963).
[8] J. A. Simpson and U. Fano, Phys. Rev. Letters, **11**, 158 (1963).
[9] J. A. Simpson, in *Proceedings of the Third International Conference on the Physics of Electronic and Atomic Collisions*, edited by M. R. C. McDowell (North-Holland Publishing Company, Amsterdam, 1964), p. 128.
[10] J. A. Simpson, C. E. Kuyatt, and S. R. Mielczarek, Rev. Sci. Instr. **34**, 1454 (1963).
[11] G. J. Schulz, in *Proceedings of the Third International Conference on the Physics of Electronic and Atomic Collisions*, edited by M. R. C. McDowell (North-Holland Publishing Company, Amsterdam, 1964), p. 124.
[12] C. E. Kuyatt, S. R. Mielczarek, and J. A. Simpson, Phys. Rev. Letters **12**, 293 (1964).
[13] J. Franck and W. Grotrian, Z. Physik **4**, 89 (1921), emphasized long ago that excited states of atoms would generally be expected to have positive affinities for electrons.
[14] The sharp rise in the inelastic cross section affects also the elastic cross section, as discussed, e.g., by A. I. Baz, Zh. Eksperim. i Teor. Fiz. **33**, 923 (1957) [English transl.: Soviet Phys.—JETP **6**, 709 (1958)].
[15] C. Ramsauer, Ann. Physik **64**, 513 (1921); **66**, 546 (1921).
[16] Reference 5, p. 5.

ments on argon show that attenuation of the electron beam outside the scattering chamber is negligible and that total-scattering cross sections can be measured in our apparatus.

The relationship between the current I_0 to the detector at zero pressure and the current I to the detector at a pressure p Torr is given by[17]

$$I(E_m)=I_0(E_m)\exp[-3.53\times10^{16}pl\sigma(E_m)], \quad (1)$$

where σ is the total-scattering cross section in cm^2, l is the path length for scattering in cm, and E_m is the mean energy of the electron beam. The cross section σ as a function of electron energy can be determined from measurements of I and I_0 as a function of energy at two different pressures. Since our purpose in most of the work we are reporting here was to locate sharp anomalies in the total-scattering cross section, we have taken little data of this type. Instead, we used an X-Y recorder to give the detector current as a function of electron energy, displaced the zero of current by an arbitrary and unknown amount, and adjusted the gain to display the resonance features as clearly as possible.

It is necessary to modify Eq. (1) when any rapidly varying features of the total-scattering cross section are distorted by the energy resolution of the electron beam, by any variations in potential along the scattering path, and by the Doppler broadening caused by the thermal motion of the gas atoms. The Doppler broadening comes from the fact that the energy of an electron with respect to an atom depends on the velocity of the atom, and this velocity is not negligibly small compared to the electron velocity. Doppler broadening has been treated by Bethe[18] in connection with neutron scattering. A Gaussian energy distribution is obtained, with a full width at half-maximum $\Delta E_{1/2}=3.338(mEkT/M)^{1/2}$. Here m and E are the mass and energy of the incident particle, and M and T are the mass and temperature of the target particles. For electron collisions there results

$$\Delta E_{1/2}=7.23\times10^{-4}(ET/M)^{1/2}, \quad (2)$$

where energies are in eV, T is in °K, and M is in atomic mass units. As an example, for helium at room temperature (300°K), perfectly monoenergetic electrons with an energy of 20 eV would have an apparent Gaussian energy distribution with $\Delta E_{1/2}=0.028$ eV. Doppler broadening distorts the total-scattering cross section by folding in a Gaussian function.

Any variations in potential along the scattering path will cause changes in electron energy which will be observed as a broadening influence on the cross section. These two effects, Doppler broadening and variations in potential, have an effect on the observed cross-section shape which is different from the effect of the electron energy distribution[19] if pressures are used in the scattering chamber which are high enough so that linear attenuation is not a good approximation. To demonstrate this point, let $g(E'-E)$ represent the combined effect of Doppler broadening and variations in potential. $[\int g(E'-E)dE'=1]$. Then the apparent cross section $\sigma_{\rm app}$ for monoenergetic electrons of energy E is given by a folding integral,

$$\sigma_{\rm app}(E)=\int g(E'-E)\sigma(E')dE', \quad (3)$$

and it is this cross section which must be used in Eq. (1). Finally, the effect of the electron energy distribution must be included. Let $I_0(E_m)f(E-E_m)dE$ represent the energy distribution of the electron current at zero pressure, where $\int f(E-E_m)dE=1$, and $I_0(E_m)$ is the total current to the detector at mean energy E_m. When the energy distribution is folded into Eq. (1), and with the apparent cross section from Eq. (3), there results

$$I(E_m)=I_0(E_m)\int f(E-E_m)\times\exp\left[-3.53\times10^{16}pl\int g(E'-E)\sigma(E')dE'\right]dE. \quad (4)$$

If the pressure p is sufficiently small, the exponential in Eq. (4) can be represented accurately by the first two terms of a power-series expansion:

$$I(E_m)=I_0(E_m)\int f(E-E_m)\times\left[1-3.53\times10^{16}pl\int g(E'-E)\sigma(E')dE'\right]dE.$$

Simplifying,

$$I(E_m)=I_0(E_m)\left[1-3.53\times10^{16}\times pl\int\int f(E-E_m)g(E'-E)\sigma(E')dE'dE\right]. \quad (5)$$

Equation (5) simply says that the absorption of electrons is linear with pressure in the low-pressure limit, and the cross section, with all broadening influences folded in, can be correctly determined. Examination of Eq. (4) shows, however, that at higher pressures the variation of current with pressure will deviate from the exponential law unless the exponential varies slowly with energy compared to the energy distribution in the electron beam. In all of the work reported here, pressures were used which caused large attentuations of the electron beam (less than 10% transmission in almost all cases), but nevertheless the attenuation was close

[17] Reference 5, p. 7.
[18] H. A. Bethe, Rev. Mod. Phys. **9**, 69 (1937), p. 140.
[19] G. J. Schulz, Phys. Rev. **136**, A650 (1964) pointed this out earlier and derived equations for a simplified case.

to exponential[9] on and off of the helium and neon resonances, giving strong indication that the energy spread of the electron beam is somewhat less than the width of the Doppler-broadened resonances. Accurate determination of resonance profiles will require that all broadening influences be reduced as far as possible and properly taken into account when evaluating attenuation data.

EXPECTED RESONANCE PROFILES

According to Fano,[20] the profile of an elastic resonance neglecting the effect of spin can be represented by the formula

$$\sigma(\epsilon)=\sigma_0[(q+\epsilon)^2/(1+\epsilon^2)]+\sigma_A, \qquad (6)$$

where $\epsilon=(E-E_{\rm res})/\frac{1}{2}\Gamma$ represents the difference of the electron energy E from the idealized resonance energy $E_{\rm res}$ in units of the resonance half-width $\frac{1}{2}\Gamma$, σ is the elastic-scattering cross section for electrons of energy E, σ_A is the nonresonant part of the cross section, $\sigma_0+\sigma_A$ is the value of σ far from the resonance, and q is a shape parameter equal to $-\cot\delta_l$ where δ_l is the scattering phase shift for the partial wave of angular momentum $l\hbar$ in which the resonance occurs. If the electron energy is greater than the lowest excitation energy of the atom, Eq. (6) is still valid but q is no longer simply related to the elastic phase shift.

The resonance profile given by Eq. (6) results in a maximum cross section $(q^2+1)\sigma_0+\sigma_A$ at $\epsilon=1/q$, and a minimum cross section σ_A at $\epsilon=-q$. The maximum cross section can also be expressed as $\pi(2l+1)\lambda\!\!\!^{-2}+\sigma_A$, where $\lambda\!\!\!^{-}=\lambda/2\pi$ and λ is the wavelength of the electron. This form is convenient, as it requires no knowledge of q. At the idealized resonance energy $E_{\rm res}$, for which $\epsilon=0$, the cross section is $q^2\sigma_0+\sigma_A$. Hence neither the maximum nor minimum cross section occurs at $E_{\rm res}$. Note that for $q\ll 1$ the minimum cross section σ_A occurs close to $E_{\rm res}$ while the maximum cross section occurs far from this energy and is not much different from $\sigma_0+\sigma_A$. For $q\gg 1$ the maximum cross section is very large and occurs close to $E_{\rm res}$ while the minimum cross section, still σ_A, occurs far from the $E_{\rm res}$. In all cases $E_{\rm res}$ is somewhere between the minimum and maximum cross sections, even though broadened as discussed above.

APPARATUS

The apparatus used to observe total-scattering resonances is shown schematically in Fig. 1. A brief description has been published,[9] and a detailed discussion is in press.[21] An electron gun forms an intense well-collimated beam which is decelerated, monochromatized by energy selection in a spherical electrostatic deflector, accelerated into the scattering chamber, decelerated, energy analyzed, reaccelerated to a Faraday cup collector, and the electron current measured with a vibrating-reed

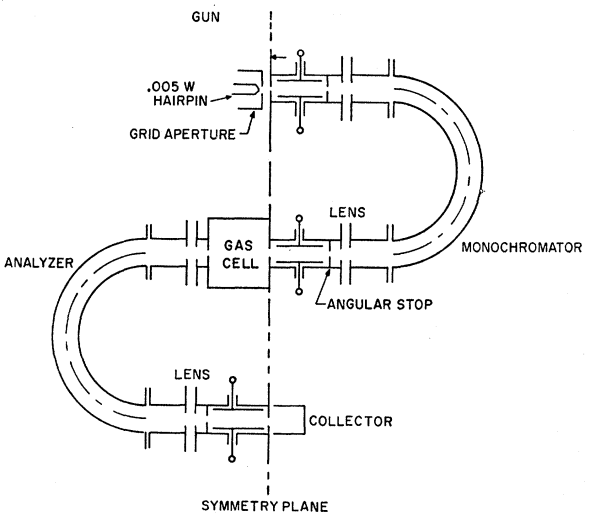

FIG. 1. Schematic diagram of apparatus.

electrometer. In contrast to the classic apparatus of Ramsauer,[15] the gas-filled scattering chamber is a separate component, and plays no role in the energy selective part of the apparatus. Differential pumping allows low pressures to be maintained in all parts of the apparatus except the scattering chamber. Gas pressures in the scattering chamber are typically in the range 0.005 to 0.1 Torr. The pressure in the remainder of the apparatus is smaller by a factor of about 200. Provision for accurate pressure measurement was not made. Angular collimation after the scattering chamber ensures that electrons which have been scattered through angles greater than $\frac{3}{4}°$ do not arrive at the collector, and the energy analyzer rejects all electrons which have lost an energy of about 0.03 eV or greater.

In operation a slowly varying voltage is used to change the electron energy in the scattering chamber. The same voltage is applied to the X axis of an X-Y recorder, while the output of the vibrating-reed electrometer is applied to the Y axis of the recorder. The curve traced out shows current to the detector as a function of applied voltage. Electron energy in the scattering chamber is equal to the applied voltage plus a constant, the constant being the so-called contact potential which involves the work function of the cathode and scattering chamber, and the particular energy slice of the electron beam selected by the monochromator. In general, this contact potential cannot be calculated but must be determined experimentally. We have used known inelastic thresholds to calibrate our energy scale for helium, and then have used the principal helium resonance as a transfer standard, as will be discussed below.

In the absence of gas in the scattering chamber, curves of current versus electron energy show a broad maximum due to the electron-optical focusing effect associated with changing the energy. Within wide limits, this broad maximum can be placed at any energy

[20] U. Fano, Phys. Rev. **124**, 1866 (1961). See also Refs. 6 and 15.
[21] J. A. Simpson, Rev. Sci. Instr. **35**, 1698 (1964).

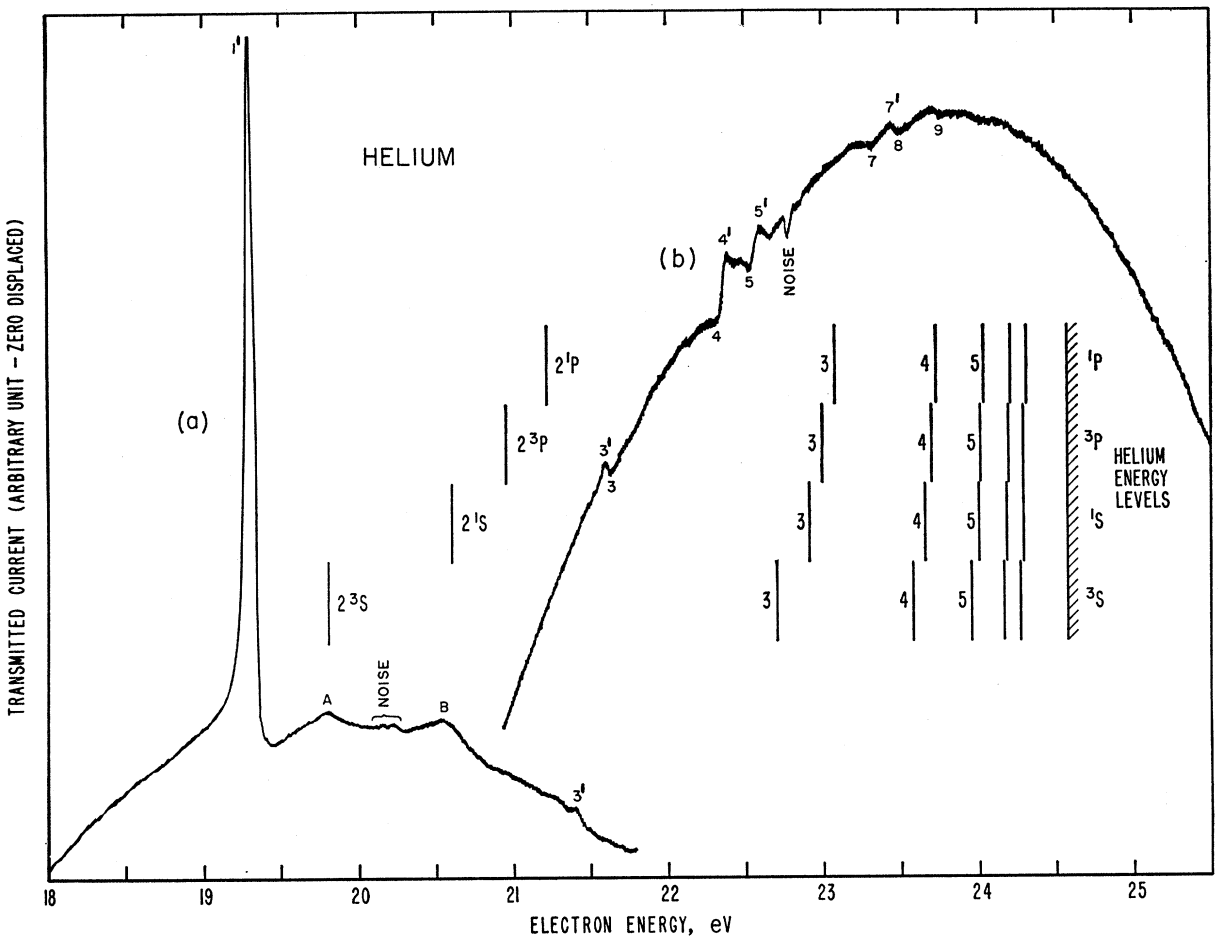

FIG. 2. Transmitted current as a function of energy for electrons in helium. Curves (a) and (b) were obtained with different adjustments of the focusing voltages in the apparatus. Resonance 3 has been observed at several energies between the two extremes shown here, while all other features show no variation greater than 0.01 eV. Also shown are some of the energy levels of the helium atom.

by adjusting the various focusing voltages available, enabling particular resonance features to be placed near the center of the broad maximum where they appear to best advantage. When using depressed zero and high recorder gain the broad maximum appears as a sharp peak with sloping sides, and this fact must be kept in mind while studying the curves presented in this paper. All curves shown are accurate tracings of unretouched X-Y recordings, except for Fig. 4 which is discussed below.

HELIUM

Figures 2, 3, and 4 show some of our recent results for helium. The resonance at 19.3 eV, labeled 1′, now appears as a striking increase in transmission in Fig. 2 [curve (a)]. The increased sensitivity and signal-to-noise level of our apparatus enabled us to detect several smaller resonances, labeled from 2 through 9 in Figs. 2–4, and a jump in transmission labeled C. Peaks in transmission are labeled with primed numbers and correspond to dips in the total-scattering cross section. Dips in transmission are labeled with unprimed numbers and correspond to peaks in the total-scattering cross section. The idealized resonance energy lies between the peak and the dip. Table I lists the energies of the dips, peaks, and other features obtained from the average of several runs.

Figure 2 [curve (a)] shows two sharp decreases in transmitted current labeled A and B, which are associated with the thresholds for exciting the $(1s2s)^3S_1$ and $(1s2s)^1S_0$ states of helium at 19.818 and 20.614 eV, respectively.[22] Figure 3 shows these inelastic thresholds with higher amplification. It must be noted that the threshold shapes may be complicated by structure in the elastic cross sections which in turn is caused by the sharp rise in the inelastic cross sections.[14] The elastic cross section should show a corresponding sharp decrease over an energy interval probably less than 0.01 eV.[23] In fact, Fig. 3 shows such an effect at the 2^3S threshold, but the

[22] Energy levels obtained from C. E. Moore, *Atomic Energy Levels*, Nat. Bur. Stds. Circular 467; Vol. I (1949); Vol. II (1952); Vol. III (1958). For conversion we took 1 $cm^{-1} = 1.23981 \times 10^{-4}$ eV.

[23] F. Prats (private communication).

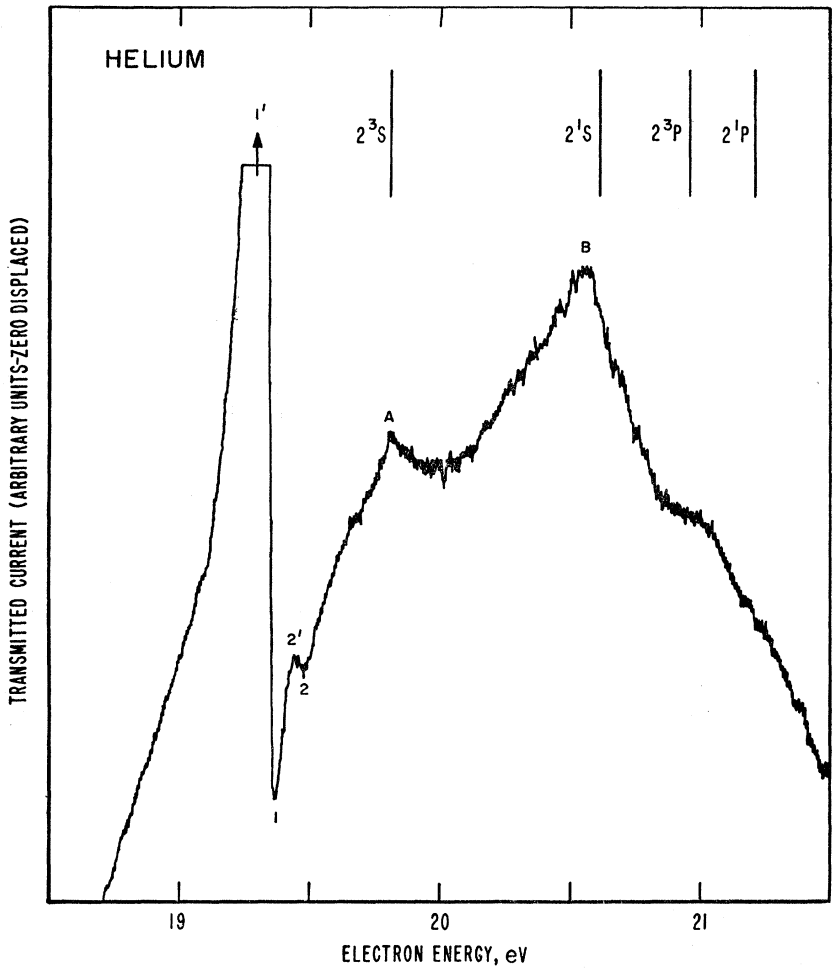

FIG. 3. Transmission of electrons by helium at energies near the lowest excited states of helium. The first four energy levels of helium are also shown.

TABLE I. Structure in transmission of electrons through helium.

Label	Type[a]	Energy (eV)[b]	
1′	Peak	19.31±0.01	$He^-(1s2s^2)^2S_{1/2}$
1	Dip	19.37±0.01	
2′	Peak	19.43±0.01	$He^-(1s2s2p)^2P^\circ$
2	Dip	19.47±0.01	
A	Break	19.818[c]	$He(1s2s)^3S_1$
B	Break	20.59±0.01	$He(1s2s)^1S_0$ (20.614 eV)
3′	Peak	21.50±0.1	
3	Dip	21.55±0.1	
4	Dip	22.34±0.02	
4′	Peak	22.39±0.02	
5	Dip	22.54±0.02	
5′	Peak	22.60±0.02	
6′	Peak	22.81±0.02	
6	Dip	22.85±0.02	
7	Dip	23.30±0.02	
7′	Peak	23.44±0.02	
8	Dip	23.49±0.02	
9	Dip	23.75±0.05	
9′	Peak	23.82±0.05	
C	Step	24.64±0.1	Onset of He^+ (24.585 eV)

[a] Type of feature in transmission.
[b] Errors quoted refer to accuracy of location relative to assumed 2^3S_1 threshold. Absolute values may be uncertain by an additional 0.02 eV.
[c] Calibration point.

measurements must be repeated before drawing definite conclusions. Since the threshold energies are known to high accuracy from spectroscopic measurements,[19] the 2^3S_1 threshold was used to determine the energy scale. We believe the resulting energy scale is accurate to ±0.03 eV, taking into account the uncertainty of the threshold shape and the precision with which features may be located. The peak transmission of resonance 1 is then found to occur at an electron energy of 19.31±0.03 eV, in excellent agreement with Schulz's value[1] of 19.3±0.1 eV for the corresponding decrease in elastic scattering at 72°. Resonance 2 is small and close to the large resonance 1 and is observed only on runs with the highest energy resolution. Resonance 3 is observed on all runs but behaves in a most remarkable manner: Its position varies from 21.4 to 21.6 eV, depending in some way on apparatus adjustment. We believe resonance 3 is a property of helium since it does not show up in runs on vacuum or on other gases. There appears to be a correlation between the position of this resonance and the angular acceptance of the energy analyzer, but further work is necessary before more

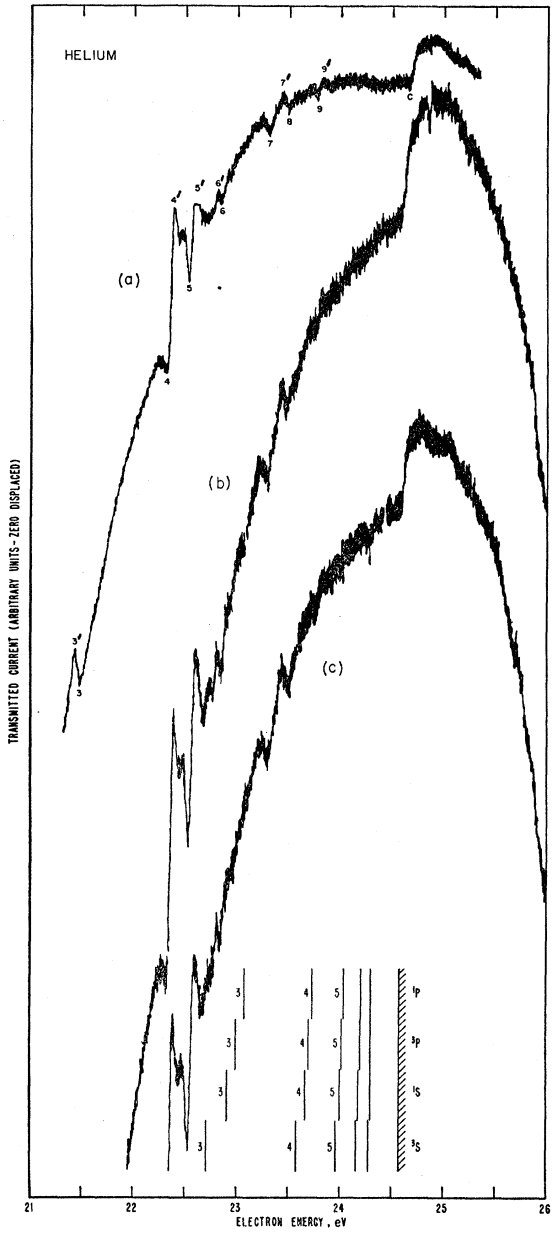

FIG. 4. Transmission of electrons by helium, showing several resonances. The vertical scale has been expanded by increasing detector gain. Curves (a), (c), and (b) were recorded with successively higher gain. Comparison of the three curves shows that the features marked on curve (a) are common to the three curves, and are not caused by noise.

definite statements can be made. Resonances 4 and 5 are also observed on all runs, while resonances 6 through 9 and the step C are observed only with the highest energy resolution and best signal-to-noise ratio. Three separate runs are shown on Fig. 4 to demonstrate that these small features are not due to noise. Curves 4(b) and (c) were obtained with about twice the gain of curve 4(a). These curves, because of depressed zero and increased gain, covered a current range greater than the vertical span of the X-Y recorder, necessitating zero changes during the runs. Due to the slow sweep speed used, these zero changes caused only very small gaps in the records. The final curves were prepared by careful alignment of the separate segments.

As interpreted by Simpson and Fano,[8] the large resonance 1 is caused by interference between formation of the $1s2s^2(^2S_{1/2})$ state of He^- and the usual potential scattering. One thinks of the $1s2s$ excited states of helium as having a positive binding energy for a third electron in the unfilled $n=2$ shell. The resonance occurs in the s-wave scattering channel. Analysis of the resonance shape by Cooper[24] gives a value for the s-wave phase shift of 100°, in close agreement with the phase shift obtained by Westin[6] from analysis of angular distributions of scattered electrons. Other resonances might be expected, involving the He^- states $1s2s2p$ ($^2P^\circ$, two distinct states) and $1s2p^2(^2S, ^2P,$ and $^2D)$. Formation of quartet states is much less likely because it requires a spin flip. Following the arguments of Fano and Cooper in the paper following this one, a p-wave electron interacting with the ground state of helium can form only ^2P states with odd parity. The ^2P configuration of $1s2p^2$ has even parity and hence can be ruled out of consideration, leaving $1s2s2p(^2P^\circ)$ and $1s2p^2(^2S, ^2D)$ as the only possibilities. The resonances associated with $(1s2s2p)^2P^\circ$ should occur in the p-wave scattering. Westin[6] obtained a p-wave phase shift of 16° at 20 eV. Thus for this resonance $q=-3.5$, and in transmission the resonance should appear as a sharp dip followed by a broad shallow peak. Resonance 2 fits this description very well.

A rough estimate of the energy of these He^- states can be made from the known energy of the doubly excited states of helium. The two excited electrons in helium are moving in a $Z=2$ field, while the two excited electrons in He^- are moving in the $Z=1$ field of He^+. Some modification is of course expected due to the $1s$ electron in He^+. The procedure is to take the energies of the doubly excited states of helium relative to He^{++} and divide by $Z^2=4$ to get the corresponding energies of the He^- states relative to He^+. Table II shows the results of such an extrapolation. The extrapolated energies are reasonable in that all of them lie within 1 eV below appropriate levels of He; the difference represents the binding energy of the third electron. The first two extrapolated He^- states coincide with the observed resonances 1 and 2. The third extrapolated He^- state has already been ruled out. The next three extrapolated He^- states lie in the region of the 2^3S, 2^1S thresholds; they have not yet been observed. The energies of several He^- states have been calculated by Wu and Shen,[25] and by Propin,[26] but the results are not sufficiently accurate for identification purposes.

[24] J. W. Cooper (private communication).
[25] T. Y. Wu and S. T. Shen, Chin. J. Phys. **5**, 150 (1944).
[26] R. Kh. Propin, Opt. i Spectroskopiya **10**, 308 (1961) [English transl.: Opt. Spectry. (USSR) **10**, 155 (1960)].

TABLE II. Correspondence between doubly excited helium and excited He^-.

Helium state	Energy (eV)	Difference from limit (eV)	Divided by $Z^2=4$ (eV)	Estimated He^- state (eV)	
$(2s^2)^1S$	57.9[a]	21.09	5.27	19.31	$(1s2s^2)^2S$
$(2s2p)^3P$	58.5[a]	20.49	5.12	19.46	$(1s2s2p)^2P^\circ$
$(2p^2)^3P$	59.66[b]	19.33	4.83	19.75	$(1s2p^2)^2P$
$(2p^2)^1D$	60.0[a]	18.99	4.75	19.83	$(1s2p^2)^2D$
$(2s2p)^1P$	60.12[c]	18.87	4.72	19.86	$(1s2s2p)^2P^\circ$
$(2p^2)^1S$	62.77[d]	16.22	4.05	20.53	$(1s2p^2)^2S$
$(sp23+)^1P$	63.65[c]	15.34	3.83	20.75	
$(sp24+)^1P$	64.46[c]	14.53	3.63	20.95	
$(3s3p)^1P$	69.95[c]	9.04	2.26	22.32	
$(sp34+)^1P$	71.66[c]	7.33	1.83	22.75	
$(4s4p)^1P$	73.77[c]	5.22	1.30	23.28	
Limit He^{++}	78.99[b]			24.58	
He^+ $2s$(or $2p$)	65.39[b]	13.60	3.40	21.18	[$He(1s2p)^1P=21.22$]
He^+ $3s$(or $3p$)	72.95[b]	6.04	1.51	23.07	[$He(1s3p)^1P=23.08$]

[a] From electron scattering, Ref. 24.
[b] From optical data, Ref. 19.
[c] From optical data, R. P. Madden and K. Codling, in *Proceedings of the Sixth International Conference of Ionization Phenomena in Gases* (Paris, 1963), p. 139.
[d] Calculated, R. Kh. Propin, Opt. and Spectry. (USSR) **8**, 158 (1960).

The resonances 4, 5, and 6 are a few tenths of an eV below the $1s3s$ and $1s3p$ states of helium. It is natural to attribute the resonances to the existence of He^- states with two electrons in the $n=3$ shell. In analogy with the resonances at lower energy, the resonance corresponding to the He^- state $(1s3s^2)^2S_{1/2}$ is expected to have the lowest energy of the group and be relatively strong since it occurs in the s-wave scattering channel. Resonance 4 appears to fit this description. Because the energy of the helium state $(3s^2)^1S$ is not known, a direct extrapolation cannot be made. Extrapolation of the known helium state $(3s3p)^1P$ does give an energy in the same neighborhood. It is more difficult to identify the states responsible for resonances 5 and 6. States such as $(1s3s4s)^2S_{1/2}$ probably do not exist. Resonance 3 is unusual in that it occurs at an energy too high to belong to the first group of resonances (it is above all $n=2$ states of helium) and at too low an energy to belong to the second group.

Resonances 7 and 8 appear to be associated with the $n=4$ states of helium, and resonance 9 with the $n=5$ states of helium. Here again, the extrapolated state $(1s4s4p)^2P$ lies very close to resonances 7 and 8.

The feature C occurs at the ionization potential of helium, to within the accuracy of our determination. It may be caused by the presence of positive ions, but there is another possibility which is more consistent with the very sharp increase in current at C. If there are series of unresolved resonances with He^+ as a limit the effect of exponential attenuation would be to change the amount of attenuation from what would be expected from the average cross section. When the limit is reached the cross section becomes smooth and the attenuation changes abruptly to the correct value. In any case, the onset of He^+ provides an independent check on the energy scale.

Some features of the 2^3S_1, 2^1S_0 threshold region merit further discussion. Using the energy scale determined from the 2^3S_1 threshold, the second break B occurs within 0.02 eV of the known excitation energy of the 2^1S_0 state. Agreement would be even closer if the small rise at the 2^3S_1 threshold were assigned to the threshold energy. Assuming that all of the significant features in the 2^3S_1, 2^1S_0 threshold region are caused by inelastic effects, a comparison can be made with the measurements of Schulz and Fox[27] for production of metastable helium atoms as a function of electron energy, and with the measurements of Schulz[28] of the total cross section for excitation of helium by electrons. Remembering that inelastically scattered electrons result in a decrease in transmitted current in our measurements, qualitative agreement is found. Both methods show sharp increases in excitation at the 2^3S_1 and 2^1S_0 thresholds, but the Schulz measurements give a 2^1S_0 threshold energy 0.1 eV too high. The excitation measurements show two peaks, at 20.4 and 21.1 eV, in qualitative agreement with the minima of transmission observed by us, although differences of the order of 0.1 eV occur in the location of these features. The higher energy resolution in our experiments probably accounts for the differences.

Baranger and Gerjuoy[29] found that the experimental results of Schulz and Fox for excitation of 2^3S can be fitted using a Breit-Wigner one-level formula, with a compound state near 20.3 eV having a width Γ of 1.0 eV. That the situation is more complicated is shown by calculations[23] which demonstrate that the $1s2s^2$ state of He^-, lying 1.1 eV below the inelastic peak, has a large effect upon it. This influence is strong because the inelastic cross section is about 1% of the elastic one.

Figure 5 shows two resonances observed in helium at considerably higher energies, 57.1 ± 0.1 eV and 58.2 ± 0.1 eV. The first of these resonances is 0.8 eV below the lowest doubly excited state of helium reported by Simpson, Mielczarek, and Cooper[30] from electron energy-loss measurements. This state of He is 57.9 eV above the ground state of helium and has been assigned the classification $(2s^2)^1S$. The second resonance is 0.3 eV below the second doubly excited state of He, $(2s2p)^3P$, at 58.5 eV. These resonances are interpreted by Fano and Cooper, in a paper[31] which immediately follows this one, in terms of temporary formation of highly excited states of He^- in which all three electrons are in $n=2$ quantum states. From consideration of the various 3-electron configurations which can be formed by electron impact on the ground state of helium, Fano and Cooper arrive at the assignments $(2s^22p)^2P^\circ$ and $(2s2p^2)^2D$ for the two resonances.

[27] G. J. Schulz and R. E. Fox, Phys. Rev. Letters **106**, 1179 (1957).
[28] G. J. Schulz, Phys. Rev. **116**, 1141 (1959).
[29] E. Baranger and E. Gerjuoy, Phys. Rev. Letters, **106**, 1182 (1957).
[30] J. A. Simpson, S. R. Mielczarek, and J. Cooper, J. Opt. Soc. Am. **54**, 269 (1964).
[31] U. Fano and J. W. Cooper, following paper, Phys. Rev. **138**, A400 (1965).

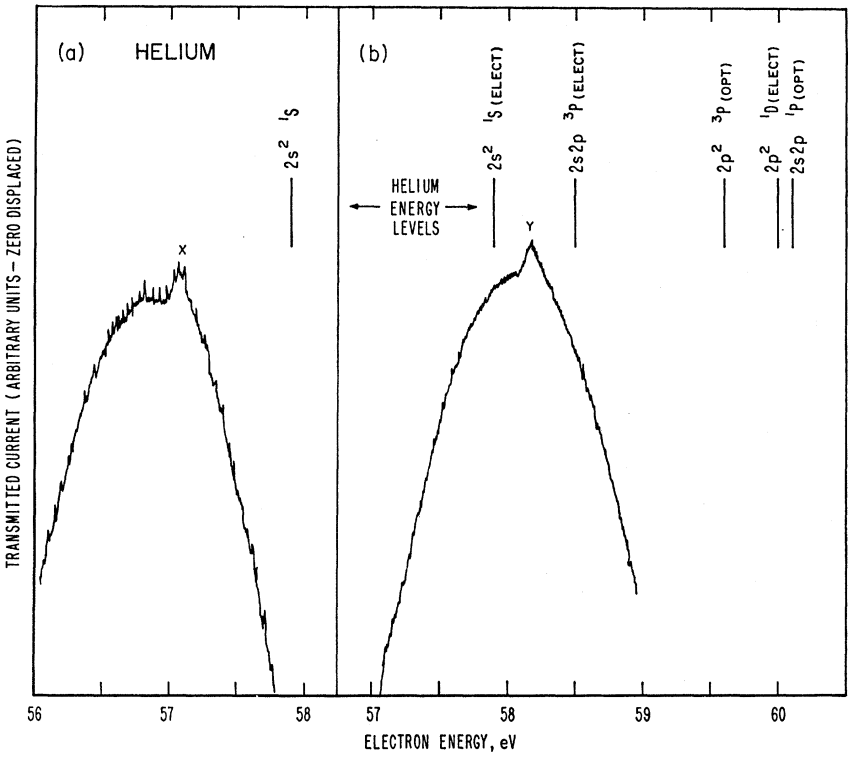

FIG. 5. Transmission of electrons by helium, showing two resonances at 57.1±0.1 and 58.2±0.1 eV. Also shown are the first few doubly excited states of helium. The labels indicate which states were obtained from electron energy loss measurements, and which from ultraviolet absorption measurements.

NEON

The two resonances previously observed in neon by Simpson[9] have now been examined with higher energy resolution and better signal-to-noise ratio, as shown by Figs. 6 and 7. These principal resonances, labeled 1 and 2, are about 0.6 eV below the first excited state of neon and appear as a pair of sharp decreases in transmission, separated by 0.095±0.002 eV. The energy scale was set first by comparing the position of the neon resonances with the position of the helium resonance in consecutive runs and then adjusted slightly (about 0.05 eV) assuming that the features marked A and B are inelastic thresholds associated with the $^3P_2$ and $^3P_0$ states of neon at 16.619 and 16.715 eV, respectively. The resulting energy scale is in good agreement with the results of Schulz[11] who measured elastic scattering in neon at 72°. Schulz, however, found only one resonance, probably due to lack of energy resolution.

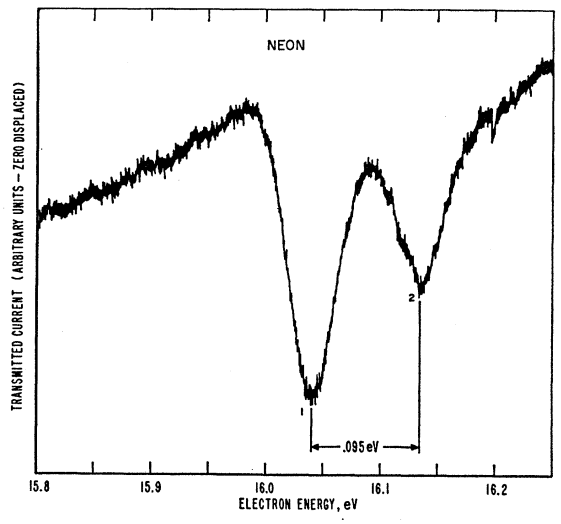

FIG. 6. Transmission of electrons by neon, showing the first two resonances located about 0.5 eV below the first excited states of neon.

Four more structures, labeled 3, 4, 5, and 6, have been observed. These are shown in Fig. 7 as they appeared in three different runs. Table III lists all of the features we have observed in neon, together with the electron

TABLE III. Structure observed in electron transmission through neon.

Feature[a]	Energy (eV)[b]
1	16.04±0.02[c]
2	16.135±0.02[c]
A	16.62±0.03
B	16.715 calibrating point
3	18.18±0.05
4	18.29±0.05
5	18.46±0.03
6	18.56±0.03

[a] Features identified on Figs. 6 and 7.
[b] Threshold B assumed to be caused by $^3P_0$ state of neon at 16.715 eV. If identification is incorrect, energy scale is uncertain by about 0.1 eV. Errors quoted refer to accuracy of relative location.
[c] Separation between 1 and 2 is 0.095±0.002 eV. Spectroscopic value of $^2P_{3/2,1/2}$ splitting in Ne^+ is 0.097 eV (Ref. 19).

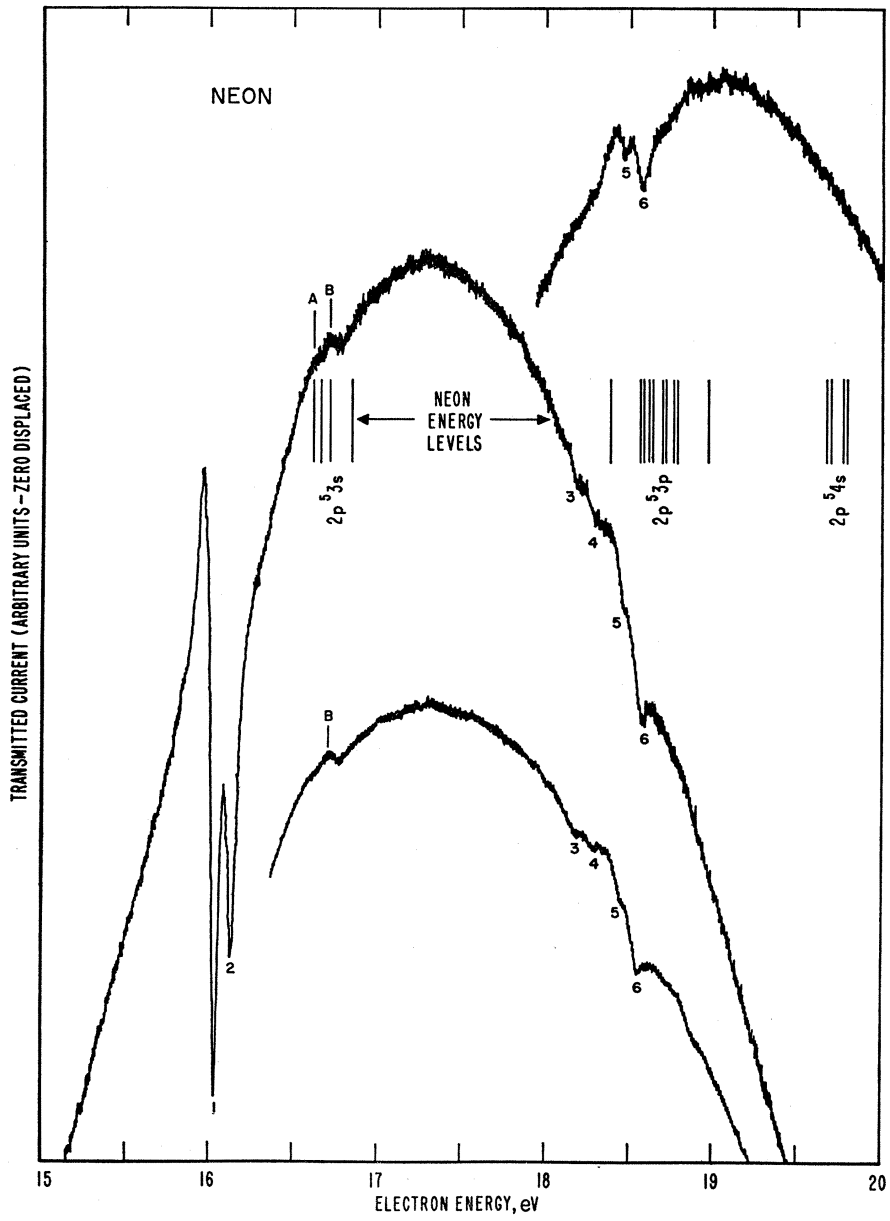

FIG. 7. Transmission of electrons by neon. Results from three separate runs are shown, together with the lowest energy levels of neon.

energies at which they occur as determined from the average of several runs. The first few energy levels of neon are shown in Fig. 7.

As interpreted by Simpson and Fano,[8] the compound states responsible for the principal neon resonances are highly excited Ne^- ions formed by adding a $3s$ electron to the lowest excited configuration of neon. The resulting configuration is $(1s^22s^22p^53s^2)^2P_{3/2,1/2}$. The spacing of the resonances agrees very well with the $^2P_{3/2}$, $^2P_{1/2}$ splitting in the ground state of Ne^+. Hence the two $3s$ electrons have very little effect on the Ne^+ core. Westin's[6] value of the p-wave phase shift for 16-eV electrons in neon is about 163°. The corresponding q is 3.5, and the cross section should show a small dip followed by a large peak, in qualitative agreement with the resonance shape we observe.

The higher structures 3 to 6 are very narrow and occur in pairs with about the same splitting as the principal resonances. We therefore believe they are resonances and are related to the $2p^53p$ states of neon. Of the possible Ne^- states which might be responsible for resonances 3 to 6, $2p^53s3p$ and $2p^53s3d$ can be ruled out since they should have energies below the $2p^53s$ neon states. Some remaining possibilities are $(2p^53p^2)^2P°$ and $(2p^53p3d)^2S$, ^2D. [The states $(2p^53p^2)^2S°$, $^2D°$ and $(2p^53p3d)^2P$ are ruled out by parity arguments.]

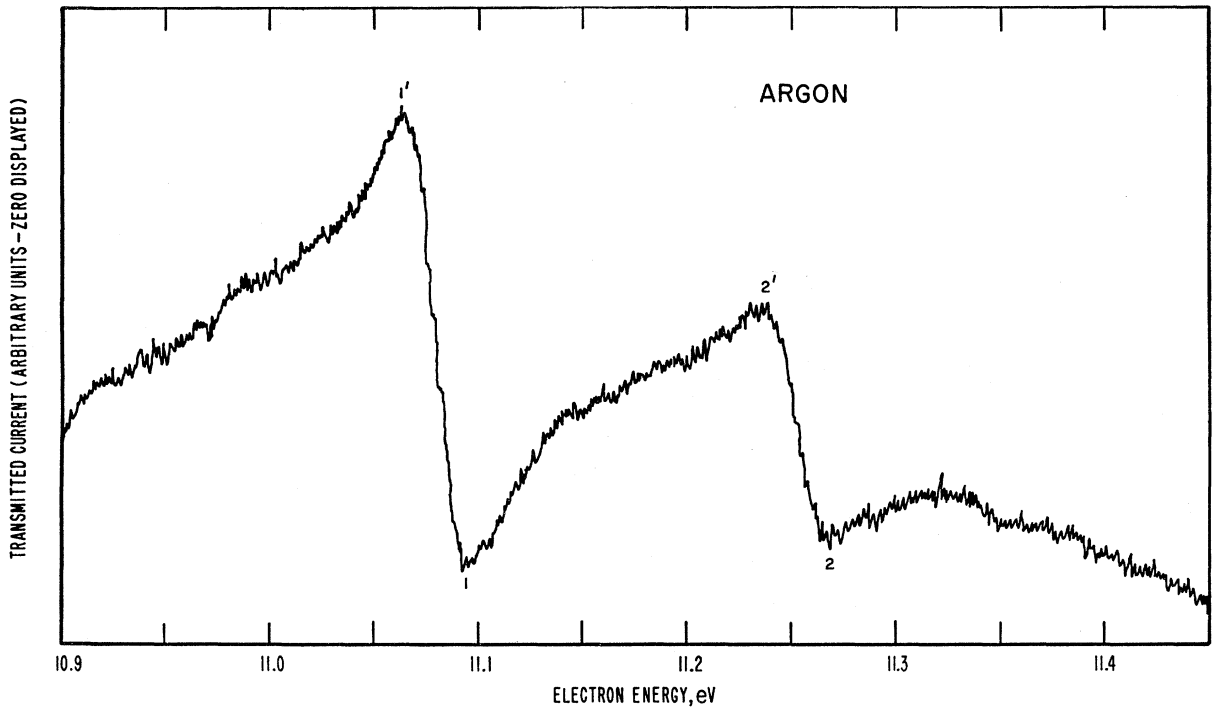

FIG. 8. Transmission of electrons by argon, showing two resonances located about 0.5 eV below the first excited state of argon.

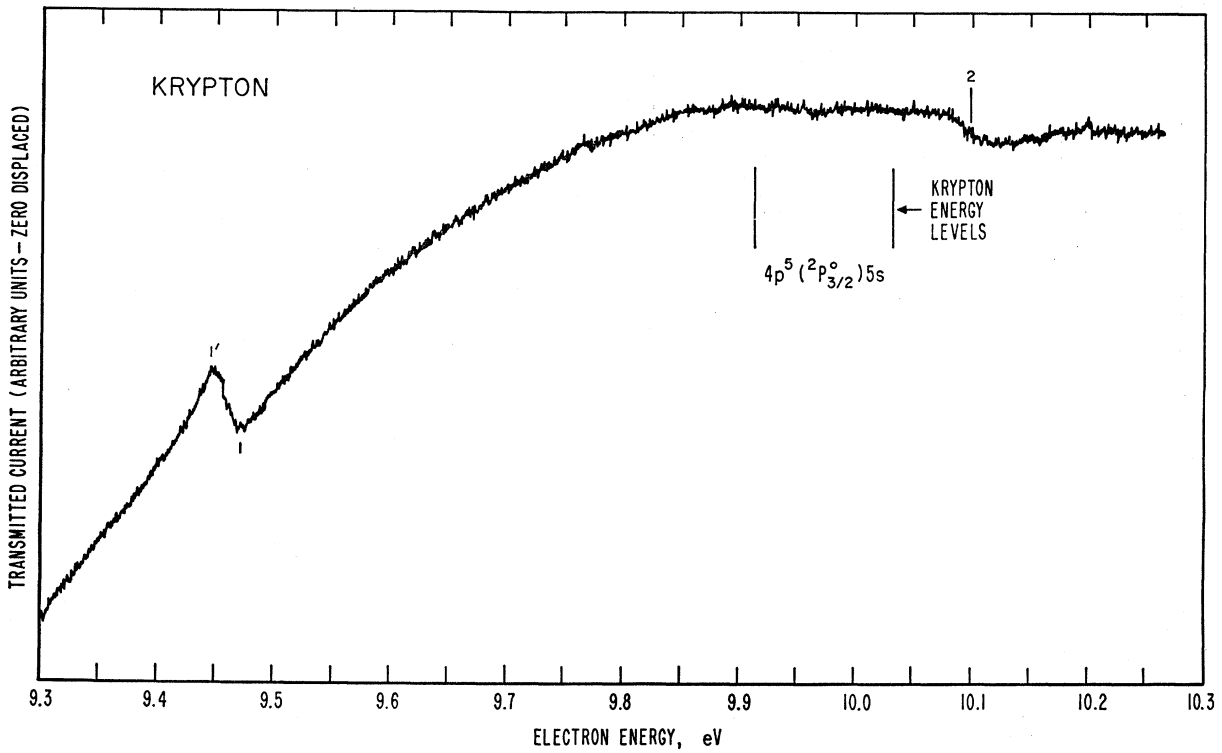

FIG. 9. Transmission of electrons by krypton, showing two resonances. The first is about 0.5 eV below the first excited state of krypton, while the second occurs at an energy above the first two excited states.

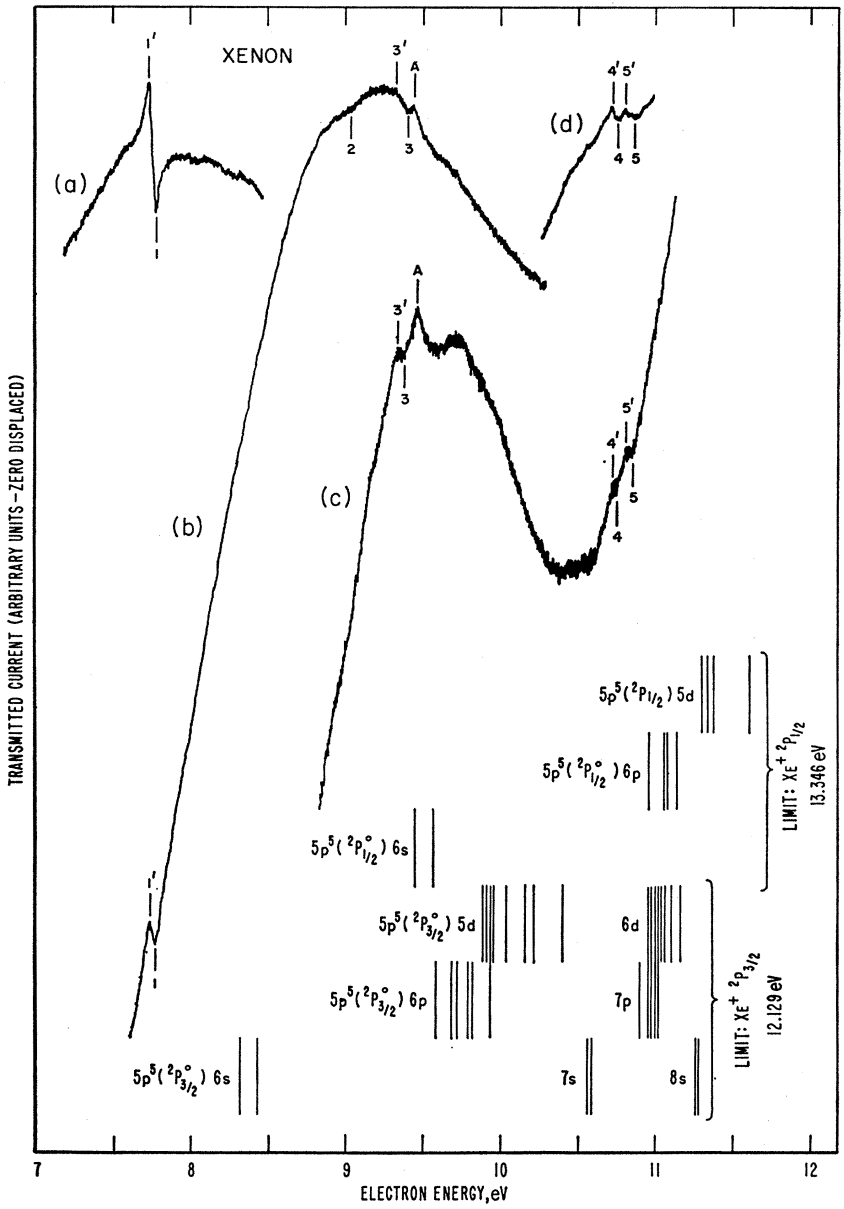

FIG. 10. Transmission of electrons by xenon, showing several resonances, the first of which is about 0.5 eV below the first excited state of xenon. Four curves are shown to illustrate all of the observed features to best advantage. An energy level diagram for xenon is also presented.

ARGON, KRYPTON, AND XENON

Figures 8–10 show the resonance structures we have observed in the heavier rare gases. In the case of xenon, portions of several runs are used to show the various features to best advantage. The energy scales were set by comparison with the helium resonance in consecutive runs. Tables IV–VI give the location of the observed features. As with neon, each gas has a pair of resonances with a separation close to the $^2P_{3/2,1/2}$ splitting of the ground-state ions. The first resonance in each gas is about 0.5 eV below the first excited state. For krypton and xenon the splitting of the resonances is great enough to place the second resonance at a higher energy than the first excited state, apparently causing appreciable broadening of the second resonance compared to the first resonance. In analogy with neon, the negative ion states are believed to be $(3p^54s^2)^2P_{3/2,1/2}$ for Ar^-, $(4p^55s^2)^2P_{3/2,1/2}$ for Kr^-, and $(5p^56s^2)^2P_{3/2,1/2}$ for Xe^-.

We have so far not observed inelastic thresholds or higher resonances in argon and krypton. Recent experiments with better signal-to-noise ratio have uncovered further structure for xenon, and we believe that future work will give similar results for argon and krypton.

Referring now to the results for xenon in Fig. 10, the structure labeled A is believed to be an inelastic threshold. The energy at which A occurs agrees to within 0.01 eV with the first of the states $5p^5(^2P_{1/2}{}^\circ)6s$. In neon the corresponding state is also believed to produce the

TABLE IV. Structure observed in electron transmission through argon.

Feature[a]	Energy (eV)[b]
1′	11.064±0.002
1	11.094
2′	11.235±0.002
2	11.267±0.003
Interval 1′, 2′	0.171±0.003[c]
Interval 1, 2	0.173±0.003[c]

[a] Features from Fig. 8.
[b] Errors quoted relative to feature 1. Additional uncertainty of ±0.05 eV applies to the over-all energy scale.
[c] Spectroscopic value of $^2P_{3/2,1/2}$ splitting in Ar^+ is 0.177 eV.[19]

TABLE V. Structure observed in electron transmission through krypton.

Feature[a]	Energy (eV)[b]
1′	9.45
1	9.48±0.01
2 (center)	10.10±0.01
Interval 1 (center), 2 (center)	0.64±0.01[c]

[a] Features from Fig. 9.
[b] Errors quoted relative to feature 1. Additional uncertainty of ±0.05 eV applies to the over-all energy scale.
[c] Spectroscopic value of $^2P_{3/2,1/2}$ splitting in Kr^+ is 0.666 eV (Ref. 19).

TABLE VI. Structure observed in electron transmission through xenon.

Feature[a]	Energy (eV)[b]
1′	7.74
1	7.77±0.01
2	9.02±0.04
3′	9.33±0.02
3	9.40±0.02
A	9.45±0.02
4′	10.71±0.02
4	10.76±0.02
5′	10.81±0.02
5	10.86±0.02
Interval 1, 2	1.25+0.05[c]

[a] Features from Fig. 10.
[b] Errors quoted relative to feature 1′. Additional uncertainty of ±0.05 eV applies to the over-all energy scale.
[c] Spectroscopic value of $^2P_{3/2,1/2}$ splitting in Xe^+ is 1.306 eV (Ref. 19).

strongest inelastic feature in the transmission curves. Similar measurements in argon and krypton are needed to provide further evidence, since the feature A can also be interpreted as a resonance giving a peak in transmission and with a half-width of about 0.1 eV.

Features 3, 4, and 5 are believed to be resonances corresponding to negative ions formed from higher excited states of xenon. Some of these excited states are shown on Fig. 10.

MERCURY

We have observed many total-scattering resonances in mercury, all of which appear as relatively sharp decreases in transmission. Some of our best runs are shown in Figs. 11–13. Resonances which are well resolved are numbered from 1 to 13 and the corresponding energies are given in Table VII. The feature marked A is a possible inelastic threshold. Its position coincides with the lowest excited state of mercury, $(6s6p)^3P_0°$. [The ground state of mercury is $(5d^{10}6s^2)^1S_0$.] Resonances 1, 2, and 3 are discussed by Fano and Cooper[31] in a paper immediately following this one. According to their analysis, these resonances correspond to the $(6s6p^2)^4P_{1/2,3/2,5/2}$ states of Hg^-, and feature 3 is a resonance, even though it occurs at nearly the same energy as the mercury state $(6s6p)^3P_1°$.

The resonances at higher energy in mercury probably lie too high in energy to be attributed to higher energy levels of the $6s6p^2$ configuration, namely, ^2D, ^2S, ^2P. It seems unlikely that the resonances at higher energy correspond to Hg^- states such as $6s7p^2$ or $6s7s7p$, since the location of the resonances appears uncorrelated

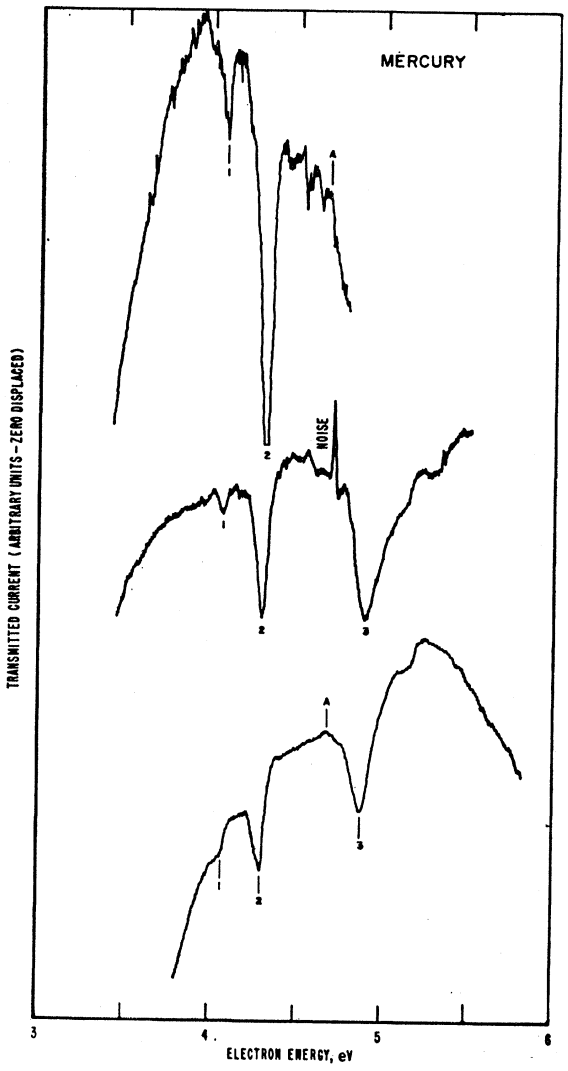

FIG. 11. Transmission of electrons by mercury vapor, showing resonances 1 to 3, and a possible inelastic threshold A.

TABLE VII. Structure observed in electron transmission through mercury.

Feature[a]	Energy (eV)[b]
1	4.07±0.01
2	4.30
A	4.68±0.02
3	4.89±0.01
4	7.81±0.05
5	7.94±0.05
6	8.14±0.05
7	8.22±0.05
8	8.83±0.05
9	8.99±0.05
10	9.75±0.05
11	10.29±0.05
12	10.58±0.05
13	10.88±0.08

[a] Features from Figs. 11–13.
[b] Errors quoted relative to feature 2. Additional uncertainty of ±0.1 eV applies to over-all energy scale.

with the corresponding Hg states. (Consult Fig. 14.) They may, however, correspond to the negative ion configuration $5d^96s^26p^2$, which involves only the $n=6$ shell, but which is expected[32] to have many energy levels in the same range where resonances 4 through 13 occur. This is apparent upon examination of the energy levels of mercury shown in Fig. 14, in particular the many levels of the configuration $5d^96s^26p$.

There is a possibility that some of the mercury resonances are actually inelastic effects. Measurements of the excitation of radiation by electrons in mercury[33] give cross sections containing several sharp peaks. It was assumed[33] that the cross section for exciting each *state* in mercury has one or perhaps two sharp peaks near threshold. When observing radiation from a particular *optical transition*, cascading from higher states contributes to the radiation, and peaks in the cross sections for exciting the higher states will appear in the excitation cross section for a transition between two lower levels. This hypothesis is consistent with the observed excitation cross sections. Comparison of the excitation data with our resonance data shows that nearly all peaks in the excitation cross sections coincide with resonances. The only exception is the prominent peak at 5.5 eV in the excitation function of the 2537-Å line $[(6s6p)^3P_1 \rightarrow (6s^2)^1S_0]$. However, this peak is about 2 eV wide at half-maximum, and could easily be missed in our measurements.

Our experiments do not differentiate between elastic and inelastic events. Hence we cannot differentiate between sharp features in the elastic scattering caused by negative ion states, and sharp features in the inelastic scattering which are not caused by negative ion states. We favor the viewpoint that very sharp features in either cross section imply the existence of negative ion states.

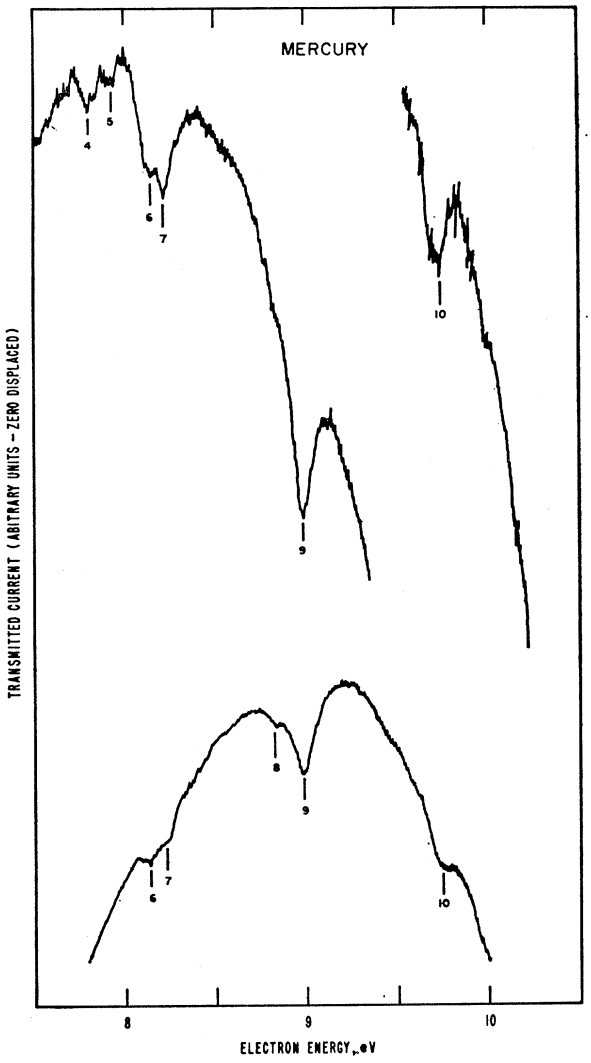

FIG. 12. Transmission of electrons by mercury vapor, showing resonances 4 to 10.

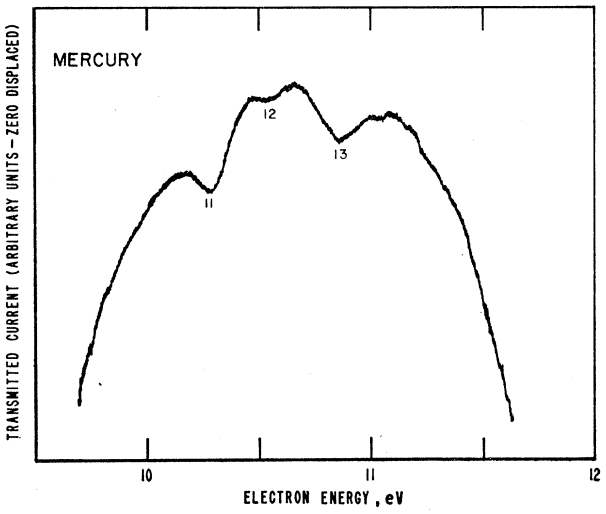

FIG. 13. Transmission of electrons by mercury vapor, showing resonances 11 to 13.

[32] N. Spector (private communication).
[33] J. A. Smit and H. M. Jongerius, Appl. Sci. Res. **B5**, 59 (1955); H. M. Jongerius, W. Van Egmond, and J. A. Smit, Physica **22**, 845 (1956); H. M. Jongerius, Philips Res. Rept. Suppl., No. 2 (1962).

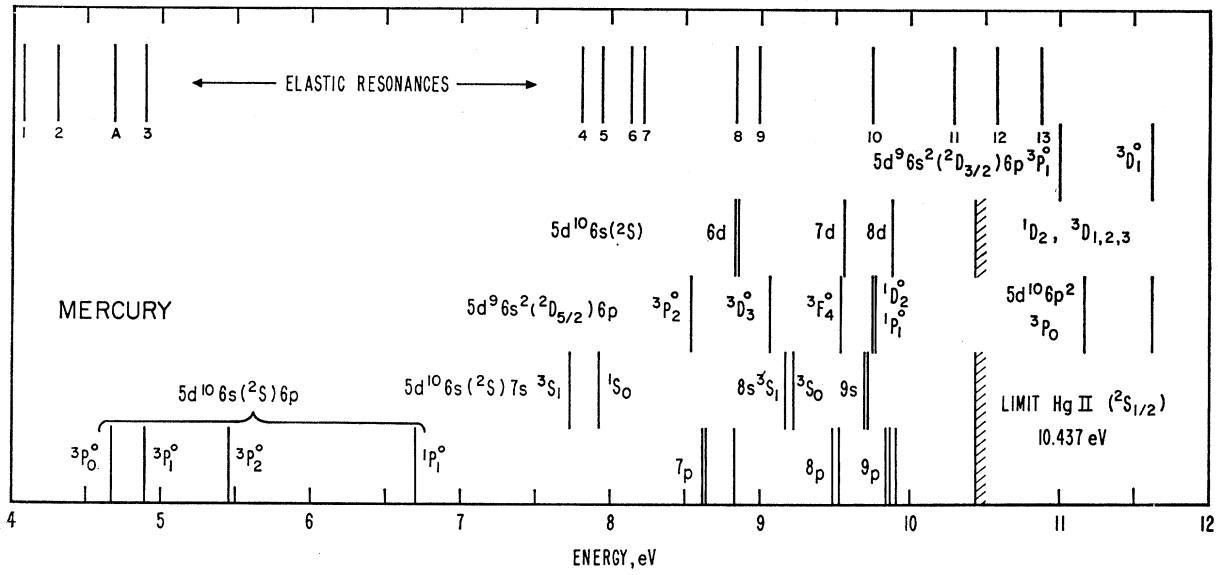

FIG. 14. Energy-level diagram of mercury. The energy at which resonances have been observed in electron transmission through mercury are shown on the top line.

CONCLUDING REMARKS

Considerable structure has been observed in electron scattering from atoms and molecules. Most of this structure is explained in terms of interference between the formation of highly excited negative ions and the more usual potential scattering. Much information is thereby obtained on the spectroscopy of negative ions, a spectroscopy which has turned out to be unexpectedly rich. Some of the structure clearly reflects the loss of electrons due to inelastic processes. Since some of these inelastic processes increase rapidly at threshold, absolute energy scales can be determined to high accuracy if the inelastic processes can be identified, and if the detailed shape of the threshold region is understood. In this way, the absolute electron energy scale for scattering in helium has been determined to 0.03 eV. Even higher accuracy should be possible by improving the energy resolution and gaining a better understanding of threshold effects. Gas-mixing experiments should enable transfer of the accurate helium energy scale to other gases.

It seems clear that all of the measurements reported here should be repeated with higher energy resolution. This we expect to do, since our apparatus has very recently been shown capable of 0.005-eV resolution.[21] Full utilization of such resolution in the lighter gases necessitates operating at very low temperatures to reduce the "Doppler" energy broadening. It is also important to measure the angular variation of the resonances, since such information is of great help in identifying the negative ion configurations.

Finally, we would urge that much more theoretical work be done on excited negative ions and their effect on inelastic scattering, particularly for helium, since much experimental evidence is already available, and it appears likely that much more will be obtained relatively soon. In contrast, many calculations have been made for atomic hydrogen, but the first resonance has yet to be experimentally observed.[34]

ACKNOWLEDGMENTS

We wish to thank Dr. U. Fano and J. W. Cooper for valuable discussions, and express our appreciation to Dr. K. Kessler, Chief of the Atomic Physics Division, for his continuing interest in this work.

[34] After this paper was prepared, G. J. Schulz reported observation of a resonance in electron transmission through atomic hydrogen. [Gaseous Electronics Conference, October, 1964 (unpublished)]. In addition, G. J. Schulz and J. W. Philbrick, Phys. Rev. Letters **13**, 477 (1964), reported measurements which show much structure in the cross section for electrons which have scattered at 72° from helium after exciting the 2^3S state. The results show that at least part of the structure observed in our measurements at the 2^1S threshold is caused by the 2^3S cross section, and that structure in the 2^3S cross section occurs in the same energy interval as our resonances 4, 5, and 6.